

## Critical Local-Moment Fluctuations, Anomalous Exponents, and $\omega/T$ Scaling in the Kondo Problem with a Pseudogap

Kevin Ingersent<sup>1</sup> and Qimiao Si<sup>2</sup>

<sup>1</sup>Department of Physics, University of Florida, Gainesville, Florida 32611-8440

<sup>2</sup>Department of Physics & Astronomy, Rice University, Houston, Texas 77005-1892

(Received 8 October 2001; published 25 July 2002)

Experiments in heavy-fermion metals and related theoretical work suggest that critical local-moment fluctuations can play an important role near a zero-temperature phase transition. We study such fluctuations at the quantum critical point of a Kondo impurity model in which the density of band states vanishes as  $|\epsilon|^r$  at the Fermi energy ( $\epsilon = 0$ ). The local spin response is described by a set of critical exponents that vary continuously with  $r$ . For  $0 < r < 1$ , the dynamical susceptibility at the critical point exhibits  $\omega/T$  scaling with a fractional exponent, implying that the critical point is interacting.

DOI: 10.1103/PhysRevLett.89.076403

PACS numbers: 71.10.Hf, 71.27.+a, 75.20.Hr, 75.40.-s

A number of stoichiometric (or nearly stoichiometric) heavy-fermion metals exhibit non-Fermi-liquid behavior when tuned to the vicinity of a magnetic quantum critical point (QCP) [1–6]. An important clue as to the nature of the quantum criticality has come from neutron scattering experiments [5,6] near the magnetic QCP of  $\text{CeCu}_{6-x}\text{Au}_x$ . At the (rather small) critical Au concentration,  $x_c \approx 0.1$ , the dynamical spin susceptibility is highly unusual in two respects: First, it satisfies  $\omega/T$  scaling. Second, the frequency and temperature dependence obeys a fractional power law, described by the same anomalous exponent over essentially the entire Brillouin zone. There are indications that the stoichiometric system  $\text{YbRh}_2\text{Si}_2$  behaves similarly [3]. These experiments directly suggest [5–9] that the fluctuations of the individual local moments are also critical. While the standard Kondo behavior of local moments in simple metals has been studied extensively over the past four decades and is well understood [10], the physics of *critical local-moment fluctuations* is largely unexplored. It is therefore highly desirable to identify models that are amenable to controlled theoretical study.

Further motivation for studying critical local-moment fluctuations comes from related theoretical work. We have recently shown [11] that competition between the Kondo and Ruderman-Kittel-Kasuya-Yosida interactions in a Kondo lattice model generates a new class of QCP, which we argue explains the aforementioned experiments in heavy fermions. Here, not only are the long-wavelength spin fluctuations critical, but so also are the local-moment fluctuations; the weight of the Kondo resonance goes to zero at the QCP. The existence of critical local fluctuations distinguishes such a “locally critical point” from the standard picture based on a spin-density-wave transition [12,13]. To fully elucidate the properties of the locally critical point, one must construct a Ginzburg-Landau description. This requires one to understand the precise nature of the critical local mode that characterizes the destruction of the Kondo effect. The first step towards

this goal is to develop an intuition about critical local-moment fluctuations in simpler models.

This paper addresses just such a model: the single-impurity Kondo problem with a power-law pseudogap. The model has a quantum phase transition at a finite Kondo coupling [14]. We show that the QCP exhibits critical local-moment fluctuations and an associated destruction of the Kondo effect very similar to those present at the locally critical point of the Kondo lattice; the local susceptibility displays  $\omega/T$  scaling with a fractional exponent. The many-body spectrum of this model can be calculated exactly, an important virtue which should significantly aid the identification of the critical local mode.

The Kondo model for a single spin- $\frac{1}{2}$  impurity coupled to a conduction band is described by the Hamiltonian,

$$\mathcal{H}_K = \sum_{\mathbf{k}, \sigma} \epsilon_{\mathbf{k}} c_{\mathbf{k}\sigma}^\dagger c_{\mathbf{k}\sigma} + \frac{J}{2} \mathbf{S} \cdot \sum_{\sigma, \sigma'} c_{0\sigma}^\dagger \boldsymbol{\tau}_{\sigma\sigma'} c_{0\sigma'} + V \sum_{\sigma} c_{0\sigma}^\dagger c_{0\sigma}, \quad (1)$$

where  $\mathbf{S}$  is the impurity spin operator,  $c_{0\sigma}^\dagger$  creates an electron with spin  $z$  component  $\sigma$  ( $= \pm \frac{1}{2}$ ) at the impurity site, and  $\boldsymbol{\tau}_{\sigma\sigma'}^i$  ( $i = x, y, z$ ) is a standard Pauli matrix.  $J$  is the Kondo exchange coupling, while  $V$  parametrizes non-magnetic potential scattering from the impurity site.

In the power-law version of this model, the conduction band is described by the (oversimplified) particle-hole-symmetric density of states [15],

$$\rho(\epsilon) = \begin{cases} \rho_0 |\epsilon|^r & \text{for } |\epsilon| \leq 1 \\ 0 & \text{for } |\epsilon| > 1. \end{cases} \quad (2)$$

In a metal ( $r = 0$ ), any antiferromagnetic Kondo coupling  $J > 0$  causes the impurity moment to be quenched at temperature  $T = 0$  [10]. With a pseudogap ( $r > 0$ ), by contrast, quenching occurs only for  $J > J_c > 0$  [14]. The

strong-coupling (i.e.,  $J > J_c$ ) and weak-coupling ( $J < J_c$ ) properties of the power-law Kondo model have been studied extensively [14,16–20]. Here, instead, we study the critical behavior at  $J = J_c(r, V)$  using numerical calculations and controlled analytical approximations. (The model appears not to be integrable [21]; it also lacks conformal invariance.) This paper supersedes an earlier preprint [22], which discussed only static critical properties, and focused on the large- $N$  limit of Eq. (1). More recent work [23] has addressed QCPs in multichannel Kondo problems with a pseudogap.

Under conditions of strict particle-hole symmetry [ $V = 0$  in Eq. (1)], a symmetric critical point (SCP) separates the weak- and strong-coupling regimes for all  $0 < r < \frac{1}{2}$ ; the strong-coupling regime and the SCP both vanish for  $r \geq \frac{1}{2}$  [17]. The SCP is also encountered away from particle-hole symmetry for  $0 < r \leq r^* \approx 0.375$ ; for  $r > r^*$ , however, there is an asymmetric critical point (ACP) distinct from the SCP [18]. In all cases, the transition can be schematically represented as shown in Fig. 1.

*Local vs impurity susceptibility.*—Our analysis begins with the observation that the quantum critical behavior reveals itself, not in the response to a uniform magnetic field  $H$ , but rather in that to a local magnetic field  $h$  coupled solely to the impurity [24,25]. These responses are measured, respectively, by the static impurity susceptibility  $\chi_{\text{imp}} = -\partial^2 F_{\text{imp}}/\partial H^2|_{H=h=0}$ , and the static local susceptibility  $\chi_{\text{loc}} = -\partial^2 F_{\text{imp}}/\partial h^2|_{H=h=0}$ , where  $F_{\text{imp}}$  is the impurity contribution to the free energy. Numerical renormalization-group (NRG) results [17,18] indicate that, whereas  $\lim_{T \rightarrow 0} T\chi_{\text{imp}}$  undergoes a jump as  $J$  passes through  $J_c$ ,  $\lim_{T \rightarrow 0} T\chi_{\text{loc}}$  goes continuously to zero as the critical coupling is approached from below, and  $\lim_{T \rightarrow 0} T\chi_{\text{loc}} = 0$  for all  $J > J_c$ . (The same distinction also holds in the large- $N$  limit [22].)

*Static critical properties.*—Given that the local field  $h$  (rather than the uniform field  $H$ ) acts as a scaling variable, we define exponents  $\beta$ ,  $\gamma$ ,  $\delta$ , and  $x$ , describing the critical behavior of the local susceptibility and the local-moment amplitude  $M_{\text{loc}} = \langle S_z \rangle = -\partial F_{\text{imp}}/\partial h|_{H=0}$ :

$$\begin{aligned} M_{\text{loc}}(J < J_c, T = 0, h = 0) &\propto (J_c - J)^\beta, \\ \chi_{\text{loc}}(J > J_c, T = 0) &\propto (J - J_c)^{-\gamma}, \\ M_{\text{loc}}(J = J_c, T = 0) &\propto |h|^{1/\delta}, \\ \chi_{\text{loc}}(J = J_c) &= C_{\text{static}} T^{-x}. \end{aligned} \quad (3)$$

Using a generalization [18] of Wilson's NRG method [26] to treat the density of states in Eq. (2), we have computed  $M_{\text{loc}}$  and  $\chi_{\text{loc}}$  for  $r$  between 0.1 and 2. For  $0 < r < 1$ , we find that  $M_{\text{loc}}$  and  $\chi_{\text{loc}}$  obey Eqs. (3) near both the SCP and the ACP, establishing the continuous nature of these phase transitions [14]. For  $r > 1$ , by contrast,  $M_{\text{loc}}$  undergoes a jump at the transition.

Table I lists exponents for the SCP, along with their estimated nonsystematic (numerical-rounding and slope-

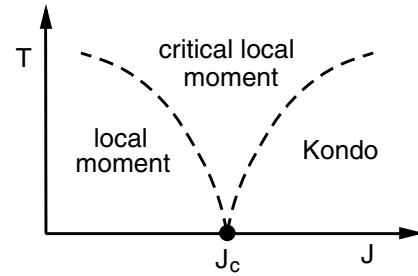


FIG. 1. Schematic phase diagram showing the vicinity of the quantum critical point of the pseudogap Kondo model.

fitting) errors. Data at  $J = J_c$  exhibit power laws over at least five decades of  $h$  and  $T$  (e.g., see  $\chi_{\text{loc}}$  vs  $T$  in Fig. 2), allowing precise determination of  $\delta$  and  $x$ . The uncertainty in  $\beta$  and  $\gamma$  is greater because rounding error cuts off the power laws as  $J$  approaches  $J_c$ . Most runs were performed for an NRG discretization parameter  $\Lambda = 9$ , retaining all states within an energy  $50T$  of the ground state [25]. To estimate the systematic discretization errors, a few runs were performed using a value  $\Lambda = 3$  lying closer to the continuum limit ( $\Lambda = 1$ ) but requiring much more computer time. Critical exponents computed for  $\Lambda = 3$  and  $\Lambda = 9$  only narrowly fail to agree within their estimated nonsystematic errors, so we believe that the  $\Lambda = 9$  exponents approximate the continuum values quite well. Restricting the power-law form of  $\rho(\epsilon)$  to a finite region around the Fermi energy to better approximate real systems does not alter the critical exponents.

The exponents listed in Table I have nontrivial  $r$  dependence. To better understand these exponents, we show that they satisfy certain hyperscaling relations, which can be derived in a standard fashion. We expect the singular component of the free energy to take the form [25]

$$F_{\text{imp}} = Tf(|J - J_c|/T^a, |h|/T^b). \quad (4)$$

Using Eq. (4), one readily finds that  $\beta = (1 - b)/a$ ,  $\gamma = (2b - 1)/a$ ,  $\delta = b/(1 - b)$ , and  $x = 2b - 1$ . These ex-

TABLE I. Properties of the symmetric critical point, obtained from NRG calculations. See the text for definitions of the exponents  $\beta$ ,  $\gamma$ ,  $\delta$ , and  $x$  (all determined using a band discretization  $\Lambda = 9$ ), and of the ratio  $R$  (calculated for  $\Lambda = 3$ ). Parentheses surround the estimated nonsystematic error in the last digit (equal to 1 where omitted).

$r$	$\beta$	$\gamma$	$1/\delta$	$x$	$R$
0.1		10.63(2)	0.005 65	0.9888	0.040(3)
0.15	0.1033(2)	7.476(2)	0.013 67	0.9730	
0.2	0.1600(2)	5.899	0.026 45	0.9485	0.17
0.3	0.3548(2)	4.441	0.0740	0.8622	
0.4	0.9140	4.018(3)	0.1852	0.6875	0.54
0.45	1.982(5)	4.335(3)	0.3134	0.5228	

TABLE II. Exponents at the asymmetric critical point, from NRG calculations using a discretization parameter  $\Lambda = 9$ . The symbols are explained in Table I.

$r$	$\beta$	$\gamma$	$1/\delta$	$x$
0.4	0.58	3.12	0.1570(2)	0.7285(5)
0.6	0.188	1.41	0.1168	0.7905(5)
0.8	0.077(2)	1.108(4)	0.0645(7)	0.8795(5)
0.9	0.039(2)	1.025(3)	0.035	0.928(2)

pressions lead to a pair of hyperscaling relations among the critical exponents, e.g.,

$$\delta = (1+x)/(1-x), \quad \beta = \gamma(1-x)/(2x). \quad (5)$$

In all cases, the exponents listed in Table I satisfy the hyperscaling relations to the accuracy of our calculations.

Table II lists critical exponents at the ACP. Comparison with Table I shows that, within their range of coexistence ( $0.375 \lesssim r < \frac{1}{2}$ ), the SCP and ACP have different exponents. For all  $r < 1$ , the hyperscaling relations, Eqs. (5), are obeyed to within estimated errors. It proves difficult to determine the critical behavior for  $r = 1$ , where there are logarithmic corrections to scaling [16]. For  $1 < r < 2$ ,  $M_{\text{loc}}$  is no longer critical, but  $\chi_{\text{loc}}$  is described by exponents  $\gamma = 2 - r$  and  $x = 1$ , values that are consistent with Eq. (4) if  $a = 1/(2 - r)$  and  $b = 1$ .

*Dynamical critical properties.*—We have also computed the imaginary part of the dynamical local susceptibility,  $\chi''_{\text{loc}}(J=J_c, \omega, T)$ . Figure 2 shows some of our zero-temperature results at the SCP. The low-frequency NRG data at both the SCP and the ACP fit the form

$$\chi''_{\text{loc}}(J=J_c, \omega, T=0) = C_{\text{dynamic}} |\omega|^{-y} \text{sgn } \omega. \quad (6)$$

For  $0 < r < 1$ , we find  $y = x$  to within numerical error, an equality that is consistent with a scaling form:  $\chi_{\text{loc}}(J=$

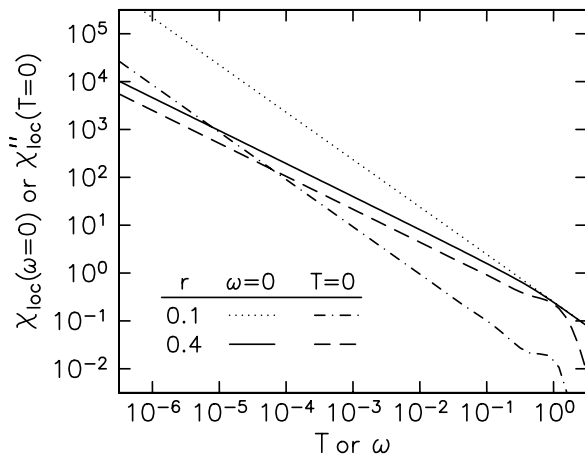


FIG. 2.  $\chi_{\text{loc}}(\omega=0)$  vs  $T$  and  $\chi''_{\text{loc}}(T=0)$  vs  $\omega$  at the symmetric critical point: NRG results for  $\Lambda = 3$ ,  $r = 0.1$  and  $0.4$  [25]. For a given  $r$ ,  $\chi_{\text{loc}}(\omega = 0, T \ll 1)$  and  $\chi''_{\text{loc}}(|\omega| \ll 1, T = 0)$  are described by equal exponents,  $x = y$ .

$J_c, \omega, T) = T^{-x} X(\omega/T)$ . Such an  $\omega/T$  scaling cannot hold for  $1 < r < 2$ , where we find  $y = \gamma < x$ .

For a given  $r$  between 0 and 1, the data for  $\chi''_{\text{loc}}(J=J_c, \omega, T)$  collapse onto a single function of  $\omega/T$ , as illustrated in Fig. 3(a). This does not conclusively establish  $\omega/T$  scaling because the NRG method is unreliable in the regime  $|\omega| \lesssim T$ . For small  $r$ , however, we can use a different approach to confirm the existence of scaling.

For small  $r$ , the local spin-spin correlation function can be calculated algebraically by a procedure analogous to the standard  $\epsilon$  expansion [27]: Since the critical coupling is small, the fixed point is accessible via an expansion in  $\rho_0 J_c \approx r$ . The unperturbed reference point ( $\rho_0 J_c = r = 0$ ) describes the standard Kondo problem, so the perturbation series for  $\chi_{\text{loc}}$  at the critical point contains logarithmic singularities. To leading logarithmic order, we find  $\chi_{\text{loc}}(\tau) = \frac{1}{4} [1 - (\rho_0 J_c)^2 \ln(\pi T \tau_0 / \sin \pi T \tau)]$ , where  $\tau_0 \approx \rho_0$ . This leads to

$$\chi_{\text{loc}}(\tau) = \frac{1}{4} \left( \frac{\pi T \tau_0}{\sin \pi T \tau} \right)^\eta, \quad \eta = (\rho_0 J_c)^2, \quad (7)$$

and to a dynamical spin susceptibility having the asymptotic low-energy, low-frequency form,

$$\chi_{\text{loc}}(\omega, T) = \frac{\tau_0^\eta \sin(\pi \eta / 2)}{2(2\pi T)^{1-\eta}} B\left(\frac{\eta}{2} - i \frac{\omega}{2\pi T}, 1 - \eta\right), \quad (8)$$

$B$  being the Euler beta function.

It follows from Eq. (8) that, for small  $r$ , the static local susceptibility and the imaginary part of the local susceptibility at  $T = 0$  have the forms specified by Eqs. (3) and (6), respectively, with exponents

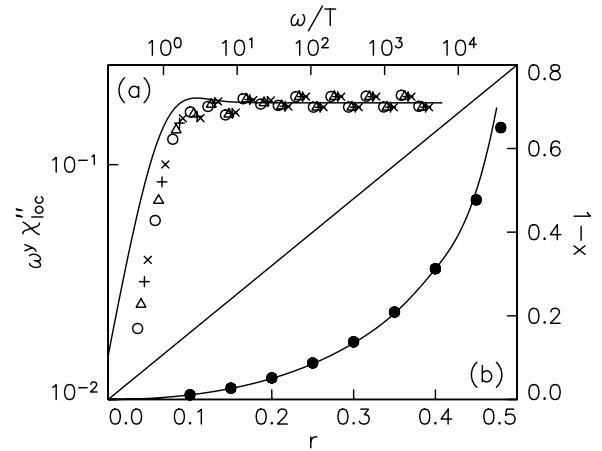


FIG. 3. Comparison between NRG and small- $r$  results for the symmetric critical point. (a)  $\omega^y \chi''_{\text{loc}}(J=J_c)$  vs  $\omega/T$  [25]: NRG results for  $r = 0.4$  and  $T/D = 10^{-7}$ ,  $10^{-6}$ ,  $10^{-5}$ , and  $10^{-4}$  (symbols) and the prediction of Eq. (8) (solid line). (b) Exponent  $1 - x$  vs  $r$ : NRG data from Table I (symbols) and the prediction of Eq. (9), in the form of a spline fit (solid line) through numerical values for  $(\rho_0 J_c)^2$ , extrapolated to the continuum limit  $\Lambda = 1$  (see [18]).

$$x = y = 1 - \eta = 1 - (\rho_0 J_c)^2, \quad (9)$$

and a universal (cutoff-independent) amplitude ratio

$$R \equiv \frac{C_{\text{dynamic}}}{C_{\text{static}}} = \frac{\pi^{2-\eta} \Gamma(1-\eta/2)}{2^\eta \sin(\pi\eta/2) \Gamma(1-\eta) \Gamma(\eta) \Gamma(\eta/2)}. \quad (10)$$

These results can be compared with our NRG data: (i) As mentioned above, we find that  $y = x$  is obeyed to the accuracy of our calculations for all  $0 < r < 1$ . (ii) The calculated  $\chi_{\text{loc}}$  obeys Eq. (8) within the range  $\omega \gg T$  where the NRG method is reliable [see Fig. 3(a)]. (iii) The numerical values of  $x$  agree remarkably well with the small- $r$  result  $x = 1 - (\rho_0 J_c)^2$ , even when  $r$  (and, hence,  $\rho_0 J_c$ ) is not small [see Fig. 3(b)]. (iv) The  $R$  values in Table I fit Eq. (10) to within 25%, a reasonable level of agreement given that the systematic errors in prefactors and critical couplings computed using the NRG are generally greater than the errors in critical exponents.

One of our key conclusions is that the dynamical spin susceptibility satisfies  $\omega/T$  scaling, as shown by Eq. (8) for small  $r$ , and supported by the equality of the exponents  $x$  and  $y$  for all  $0 < r < 1$ . This has important implications for the field-theoretical description of the QCP. It indicates that a suitably defined relaxation rate is linear in temperature, which can come about only if the Ginzburg-Landau action, written in terms of the critical local modes, contains nonlinear couplings that are relevant in the renormalization-group sense [28]. The fixed point must be interacting. For  $r > 1$ , the relaxation rate ( $\propto T^{x/y}$ ) is superlinear, which is consistent with a Gaussian fixed point.

Finally, we note that the  $r = 1$  pseudogap Kondo problem is also important for impurities in high- $T_c$  superconductors [20,29]. The quantum critical regime will likely become accessible via scanning tunneling microscopy once measurements are extended to higher temperatures.

In summary, we have combined numerical and analytical approaches to obtain a consistent picture of the critical properties of the Kondo problem with a conduction-electron density of states proportional to  $|\epsilon|^r$ . At the QCP, the weight of the Kondo resonance has just gone to zero; as a result, the local-moment fluctuations are critical. In addition, the dynamical spin susceptibility at the QCP displays  $\omega/T$  scaling with an anomalous exponent for all  $0 < r < 1$ . These features parallel those of the locally critical point in the Kondo lattice [11]. Thus, the pseudogap Kondo model provides a testing ground for studying critical local-moment fluctuations of the type seen in certain heavy-fermion metals [3–6]. The exact many-body spectrum of this impurity model can be calculated using NRG techniques, which should prove particularly useful in identifying the proper local modes for characterizing the QCP. This, in turn, should shed much new light on the Ginzburg-Landau description of the locally critical point of

the Kondo lattice. These important issues are left for future work.

We thank C. R. Cassanello, E. Fradkin, and J. W. Wilkins for useful discussions. This work has been supported in part by NSF Grant No. DMR-9316587 (K.I.), by the Robert A. Welch Foundation, NSF Grant No. DMR-0090071, Research Corporation, and TCSUH (Q.S.). Q.S. also acknowledges the hospitality of Argonne National Laboratory, the University of Chicago, and the University of Illinois at Urbana-Champaign.

- 
- [1] N. D. Mathur *et al.*, Nature (London) **394**, 39 (1998).
  - [2] H. v. Löhneysen *et al.*, Phys. Rev. Lett. **72**, 3262 (1994).
  - [3] O. Trovarelli *et al.*, Phys. Rev. Lett. **85**, 626 (2000).
  - [4] G. Stewart, Rev. Mod. Phys. **73**, 797 (2001).
  - [5] A. Schröder *et al.*, Nature (London) **407**, 351 (2000); Phys. Rev. Lett. **80**, 5623 (1998).
  - [6] O. Stockert *et al.*, Phys. Rev. Lett. **80**, 5627 (1998).
  - [7] P. Coleman, Physica (Amsterdam) **259B–261B**, 353 (1999); P. Coleman, C. Pépin, Q. Si, and R. Ramazashvili, J. Phys. Condens. Matter **13**, R723 (2001).
  - [8] Q. Si, J. L. Smith, and K. Ingersent, Int. J. Mod. Phys. B **13**, 2331 (1999).
  - [9]  $\omega/T$  scaling is also observed in the strongly disordered UCu<sub>5-x</sub>Pd<sub>x</sub>: M. C. Aronson *et al.*, Phys. Rev. Lett. **75**, 725 (1995); D. E. MacLaughlin *et al.*, *ibid.* **87**, 066402 (2001).
  - [10] A. C. Hewson, *The Kondo Problem to Heavy Fermions* (Cambridge University Press, Cambridge, England, 1993).
  - [11] Q. Si, S. Rabello, K. Ingersent, and J. L. Smith, Nature (London) **413**, 804 (2001); cond-mat/0202414.
  - [12] J. Hertz, Phys. Rev. B **14**, 1165 (1976).
  - [13] A. J. Millis, Phys. Rev. B **48**, 7183 (1993).
  - [14] D. Withoff and E. Fradkin, Phys. Rev. Lett. **64**, 1835 (1990).
  - [15] All energies are expressed in units of the half bandwidth and measured from the Fermi energy,  $\epsilon = 0$ .
  - [16] C. R. Cassanello and E. Fradkin, Phys. Rev. B **53**, 15 079 (1996); **56**, 11 246 (1997).
  - [17] K. Chen and C. Jayaprakash, J. Phys. Condens. Matter **7**, L491 (1995).
  - [18] C. Gonzalez-Buxton and K. Ingersent, Phys. Rev. B **57**, 14 254 (1998), and references therein.
  - [19] R. Bulla, M. T. Glossop, D. E. Logan, and T. Pruschke, J. Phys. Condens. Matter **12**, 4899 (2000).
  - [20] M. Vojta and R. Bulla, Phys. Rev. B **65**, 014511 (2002).
  - [21] N. Andrei (private communication).
  - [22] K. Ingersent and Q. Si, cond-mat/9810226.
  - [23] M. Vojta, Phys. Rev. Lett. **87**, 097202 (2001).
  - [24]  $H$  and  $h$  enter the Hamiltonian through an additional term  $\mathcal{H}_{\text{mag}} = \sum_{\sigma} [(H + h)S^z + (H/2) \sum_{\mathbf{k}} c_{\mathbf{k}\sigma}^{\dagger} \tau_{\sigma\sigma}^z c_{\mathbf{k}\sigma}]$ .
  - [25] We employ units in which  $\hbar = 1$ ,  $k_B = 1$ , and  $g\mu_B = 1$ .
  - [26] K. G. Wilson, Rev. Mod. Phys. **47**, 773 (1975).
  - [27] K. G. Wilson and J. Kogut, Phys. Rep. C **12**, 75 (1974).
  - [28] S. Sachdev, *Quantum Phase Transitions* (Cambridge University Press, Cambridge, England, 1999).
  - [29] A. Polkovnikov, S. Sachdev, and M. Vojta, Phys. Rev. Lett. **86**, 296 (2001); J.-X. Zhu and C. S. Ting, Phys. Rev. B **63**, 020506 (2001).